Selective silver atom interaction at β-SiC(100) surfaces: From anisotropic diffusion to metal atomic wires and stripes

M. D'angelo, V. Yu. Aristov,* and P. Soukiassian

*Commissariat à l'Energie Atomique, Laboratoire SIMA, DSM-DRECAM-SPCSI, Bâtiment 462, Saclay,
91191 Gif sur Yvette Cedex, France
and Département de Physique, Université de Paris-Sud, 91405 Orsay Cedex, France*
(Received 5 April 2007; published 5 July 2007)

Silver (Ag) atom interaction on β-SiC(100) surface reconstructions is investigated by atom-resolved scanning tunneling microscopy. On the 3×2 (Si-rich) reconstruction, the adsorbate-adsorbate interaction is dominant with no surface wetting, leading to Ag cluster formation. In contrast, on the $c(4 \times 2)$ Si-terminated reconstruction, almost equivalent Ag-Ag and Ag-surface interactions allow selective one dimensional nanoobject formation including Ag atomic wires and stripes following the substrate registry. Their orientation is mediated by anisotropic Ag atom diffusion occurring along Si-dimer rows at 25 °C and perpendicularly to them at elevated temperatures, suggesting dimer flipping as diffusion barrier. These metal nanowires potentially open up cross-wiring capability in massively parallel Si atomic lines network.

I. INTRODUCTION

Atom diffusion on surfaces is of central interest since it is at the origin of surface organization, adsorbate ordering, nano-object formation, and more generally, self-organization mechanisms. Silver adsorption on surfaces is a model system because of the very delicate balance between adsorbate-adsorbate vs adsorbate-substrate interactions, which very much depend on the substrate nature and properties. This topic was already of strong interest centuries ago, e.g., for the manufacture of mirrors. Indeed, on insulators such as oxides or glass that are very important from the applications point of view, Ag tends to form three dimensional (3D) clusters because of a dominant Ag-Ag interaction with no surface wetting in normal conditions.[1] In contrast, Ag interaction with a metal substrate generally leads to alloy formation as a result of strong Ag interaction with the surface.[2] The situation with semiconductor surfaces looks just between these two, with Ag-Ag and Ag-surface interactions being rather close with no alloy formation like for silicon surfaces unlike other full d-band metals such as Cu.[3–8] Similarly, II-VI compound semiconductor surfaces tend to be not reactive with full d-band metals such as Au but reactive with, e.g., Al.[9] Instead, reactive interface formation occurs with Ag or Au on polar surfaces of III-V compound semiconductors.[10–12] Ag adsorption has been widely investigated on silicon surfaces with many interesting issues and exotic properties.[3–8] In these views, Ag interaction with wide band gap semiconductor surfaces is of interest, especially for transport property of Ag nanostructures because of the expected minimization of bulk contribution to the conductivity.[8]

Silicon carbide (SiC) is a ceramic and a IV-IV compound wide band gap semiconductor, with band gap ranging from 2.4 to 3.3 eV depending on the polytype.[13] It is only recently that the atomic control and understanding of SiC surfaces have been achieved for both cubic (β) and hexagonal (α) phases,[14–16] opening up the possibility of investigating adsorbate interaction with atomically controlled and well-defined surfaces. Another unique feature of β-SiC(100) surface is the self-fabrication of highly stable massively parallel Si

atomic lines forming a neural architecture.[16–19] In addition, metallic Ohmic contact with these atomic Si lines has been successfully achieved by a lithography process using a transition metal, niobium.[19] The β-SiC(100) surface has up to ten different surface reconstructions[16] including two of special interest in the present study, the Si-rich 3×2 (Refs. [16] and [20–23]) and the Si-terminated $c(4 \times 2)$.[16,24–29] Their atomic structures have been determined by different experimental techniques including scanning tunneling microscopy (STM), grazing incidence x-ray diffraction, photoelectron diffraction, and *ab initio* total energy and grand canonical calculations.[16,20–27,29] The strain driven atomic structure of the Si-rich β-SiC(100) 3×2 surface reconstruction includes three Si atomic planes on top of the first C layer in a two-adlayer asymmetric dimer, alternately long and short dimers model.[16,20–23] Instead, the Si-terminated β-SiC(100) $c(4 \times 2)$ surface reconstruction, which is also strain driven, has an organization that includes dimer rows having alternating up and down dimers (AUDDs).[16,24–27,29] In contrast to the 3×2 reconstruction, the $c(4 \times 2)$ surface has its topmost Si plane located just above the first carbon atomic layer, leading to a more polar surface.[24]

Metal interaction on SiC surfaces has been studied primarily in the thin film regime with only two of such investigations for Ag.[30,31] As far as we know, there is no atomic-scale investigation of Ag-SiC systems, despite the great interest in comparing Ag interaction on silicon carbide surfaces with corresponding silicon surfaces. Among the important issues, possible Ag atom diffusion onto β-SiC(100) surfaces is of interest since its control may lead to specific adsorbate atomic organization and novel nanostructure fabrication. However, there are only two of such investigations on Ag atom surface diffusion performed for the Si(100) 2×1 surface, both using *ab initio* theoretical calculations with no available atomic-scale experimental study.[32,33] Furthermore, these two theoretical studies predict opposite views for Ag atoms on Si(100) with an anisotropic diffusion perpendicular to the Si-dimer rows in one case[32] vs an isotropic diffusion in the other case.[33] So far, no similar investigation for silicon carbide surfaces is available.

In this article, we study Ag atom interaction with the β-SiC(100) 3×2 and $c(4\times2)$ surfaces by atom-resolved STM. No on-site adsorption occurs on the 3×2 reconstruction with 3D Ag cluster formation and no surface wetting. In strong contrast, Ag atoms follow the $c(4\times2)$ surface registry with pedestal adsorption sites. A highly anisotropic Ag atom diffusion occurs along the dimer rows which act as atomic "railways" at 25 °C and perpendicularly at elevated temperatures (600 °C), allowing the formation of one dimensional Ag atomic wires and stripes that can be used as bridging nanocontacts between Si atomic lines forming a neural network.

II. EXPERIMENTAL DETAILS

The STM experiments are performed at pressures below 5×10^{-11} torr using an Omicron VT-STM. We use single domain β-SiC(100) thin films prepared at CRHEA (CNRS, Sophia Antipolis) on a 4° vicinal Si(100) surface by C_3H_8 and SiH_4 chemical vapor deposition. High quality β-SiC(100) $c(4\times2)$ and 3×2 surface reconstructions are routinely prepared from sequences of thermal annealing and Si deposition from a carefully outgassed silicon source. These procedures result in very reproducible and clean surfaces, as confirmed by sharp single domain low energy electron diffraction patterns. Furthermore, the very low pressure used during the experiments allows us to keep a stable $c(4\times2)$ surface reconstruction (well known to be especially highly sensitive to background contamination) during a complete set of measurements. Research grade Ag deposition onto the β-SiC(100) surface is performed at room temperature. The Ag coverage is determined through the Ag-Si surface atom ratio as identified by atom-resolved STM. Notice that in the STM topographs for the $c(4\times2)$ surface reconstruction, one spot of the clean surface identifies a Si-Si up dimer when tunneling in the filled electronic states, while the down dimer remains hidden to the STM tip.[24,25] This means that one spot in the STM topograph indicates the presence of two Si atoms plus two other Si atoms corresponding to the hidden down dimer.[24,25] This is taken into account when determining the Ag coverage of the β-SiC(100) $c(4\times2)$ surface. Other experimental details about high quality β-SiC(100) surface preparation are available elsewhere.[16,20,22–25,28,29]

III. RESULTS

We first look at the effect of a small amount of Ag deposition on the Si-rich 3×2 and Si-terminated $c(4\times2)$ reconstructions. Figure 1(a) displays a 210×210 Å^2 STM topograph (filled electronic states) of a β-SiC(100) 3×2 surface.[16,20] Most of the surface remains unaffected by Ag deposition. However, bright spots (not present on the clean surface) near defect sites indicate 3D Ag cluster formation having various sizes from 7 to 50 Å. Turning to the $c(4\times2)$ reconstruction, Fig. 1(b) exhibits a 260×260 Å^2 filled state STM topograph for the same deposited Ag amount (corresponding to an Ag coverage at $\theta\approx3\%$). In strong contrast to the 3×2, there is no Ag cluster formation with Ag atoms
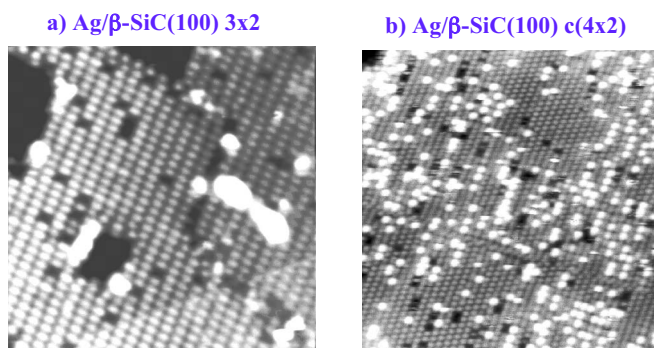

a) Ag/β-SiC(100) 3x2   **b) Ag/β-SiC(100) c(4x2)**

FIG. 1. (Color online) STM topographs (filled states) of (a) 0.3 ML Ag/β-SiC(100) 3×2 (210×210 Å^2) and (b) 0.3 ML Ag/β-SiC(100) $c(4\times2)$ (260×260 Å^2). $V_S=-3$ V, $I_t=0.3$ nA.

individually adsorbed at specific sites. The Ag atoms appear as bright spots all over the surface while the well known pseudohexagonal pattern of β-SiC(100) $c(4\times2)$ surface reconstruction[16,24,25] is seen in the areas not covered by Ag. So, while Ag-Ag interactions seem dominant on the 3×2 surface, the situation differs for the $c(4\times2)$, with Ag-Ag and Ag-surface interactions being comparable. Ag atoms follow the substrate registry, indicating its influence on adsorbate ordering. Also, Ag atoms are preferentially aligned along dimer rows. Indeed, if we look at the Ag chain total length along the directions parallel and perpendicular to the dimer rows, we find 70% of the Ag atoms aligned along the dimer rows. Besides, having more than two Ag atoms aligned perpendicularly to dimer rows represents only 22% of the cases.

In order to identify Ag atom adsorption sites at this low coverage, we show in Fig. 2(a) a more detailed 50×55 Å^2 STM topograph. By a visual inspection, one can clearly see Ag atoms adsorbed on the dimer rows and not between them, leaving three options only for the adsorption, the bridge on top of (i) an up or (ii) a down Si dimer, and (iii) the pedestal (between an up and a down dimer) sites. To discriminate
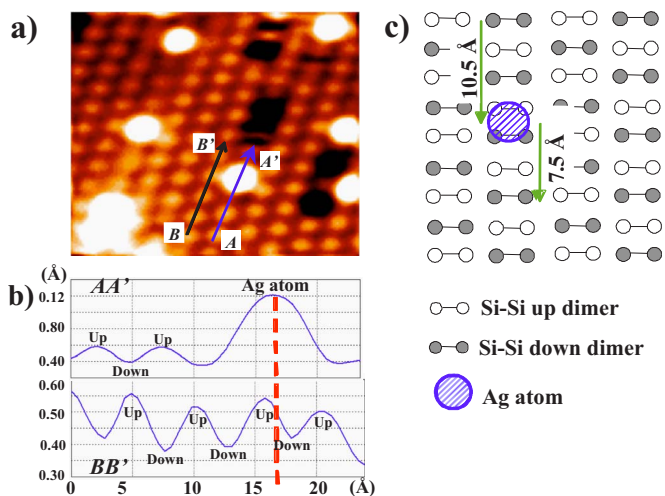

FIG. 2. (Color online) (a) 50×55 Å^2 zoom picture of Fig. 1(b) for Ag/β-SiC(100) $c(4\times2)$. (b) Height profile plots along dimer rows with (AA′) and without BB′ a Ag atom. (c) Schematic model of Ag adsorption site on the β-SiC(100) $c(4\times2)$ surface.
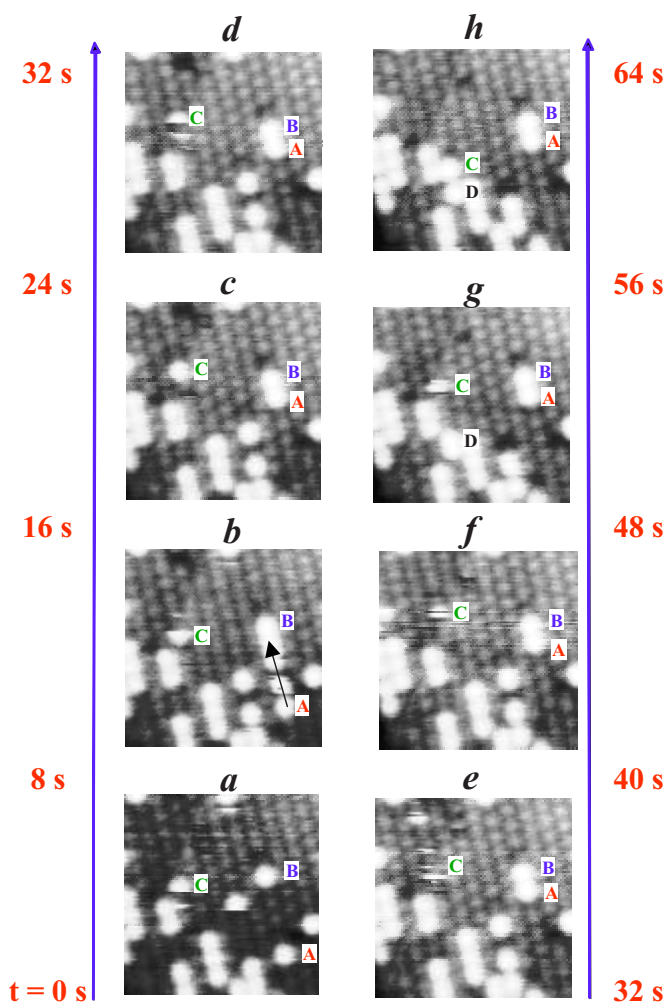
FIG. 3. (Color online) Sequence of eight filled states STM topographs (70×70 Å^2) showing Ag atom migration along the Si-dimer rows on the β-SiC(100) $c(4 \times 2)$ surface from 0 to 64 s. V_S =-3 V, I_t=0.3 nA.

FIG. 4. (Color online) (a) 410×480 Å^2 STM topograph (filled states) showing Ag stripe formation and (b) 140×70 Å^2 STM topograph showing Ag atomic wire formation along the $\langle 110 \rangle$ direction after annealing around 600 °C of a 1 ML of Ag/β-SiC(100) $c(4 \times 2)$ surface. V_S=-5 V, I_t=0.37 nA.

between these three possible sites, we plot two height profiles along two adjacent dimer rows with only one having an adsorbed Ag [Fig. 2(b), top and bottom]. As can be seen, the Ag atom is not located on top of a dimer (up or down). Actually, the distance between two neighbor up dimers belonging to the same row is 6.16 Å, while the distances between the Ag atoms and the two closer up dimers are 1.54 and 4.62 Å. This means the Ag atoms are adsorbed between up and down dimers (1.54 Å being half the distance between up and down dimers at 3.08 Å), in a pedestal site, as shown in Fig. 2(c). Such an adsorption site could favor hybridization between Ag 5s extended orbitals with more localized Si 3p dangling bonds favoring a weak covalent bonding, as for alkali metals on semiconductor surfaces also having one valence electron.[34]

Another interesting aspect of Ag interaction with the $c(4 \times 2)$ surface is found by exploring the dynamics of Ag atoms and time dependence behavior at room temperature. Figures 3(a)–3(h) show a sequence of eight 70×70 Å^2 STM topographs recorded continuously for the same surface area for 64 s. Some Ag atoms are seen moving along dimer rows. We
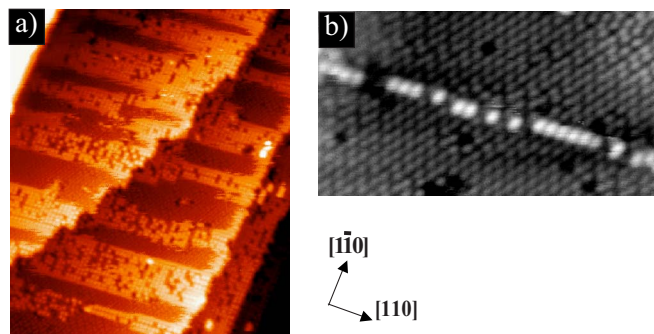
follow the motion of a Ag atom labeled A. From Figs. 3(a) and 3(b), A is moving towards Ag atom B along the Si-dimer row, as can be seen from a series of A "phantom spots" captured by the STM tip during scanning. In Fig. 3(c), A reaches B, keeping this neighbor adsorption site for 64 s [Fig. 3(h)] up to 196 s (not shown here). The A_{Ag}-B_{Ag} distance is 6.4 Å, i.e., $\approx 2 \times 3.08$ Å, the surface lattice parameter, leaving an unoccupied pedestal site between them. We make similar observations for other Ag atoms such as C moving toward and joining D between 56 and 64 s [Fig. 3(h)].

We should emphasize that Ag atom motions along a dimer row are not due to the STM tip since the scanning direction is perpendicular to the Ag diffusion direction. The anisotropic motion of Ag atoms on the β-SiC(100) $c(4 \times 2)$ surface indicates a lower diffusion barrier along the Si-dimer rows, in contrast to the behavior predicted by theory for Ag-Si(100) 2×1 surface with either a lower diffusion barrier perpendicular to the dimer rows,[32] or an isotropic diffusion for the Ag atoms.[33] However, one should notice that, in the latter calculations, Ag-Ag dimer formation is predicted to occur at higher coverages with an anisotropic diffusion between the Si-dimer rows.[33]

It is now challenging to explore temperature effects on Ag atom diffusion by first looking at a 1 ML (monolayer) Ag/β-SiC(100) $c(4 \times 2)$ surface. After annealing above 600 °C, most of the Ag atoms are desorbed. Most interestingly, remaining Ag atoms are seen to self-organize in one dimensional (1D) nanostructures ranging from Ag stripes to Ag single isolated atomic wire, as can be seen in Figs. 4(a) and 4(b). Amazingly, these 1D Ag nanostructures are perpendicular to the Si-dimer rows of the $c(4 \times 2)$ reconstruction (the [$1\bar{1}0$] direction), i.e., perpendicular to the preferential direction of Ag atom alignment at room temperature, suggesting a very different ordering mechanism. The same trend is also observed when Ag deposition is performed at a lower surface temperature of 300 °C, preventing Ag atom desorption while favoring self-organization. Figure 5(a) shows such a 1 Ag ML covered $c(4 \times 2)$ surface also having one Si atomic line along the [$1\bar{1}0$] direction.[16–18] Interestingly, the Ag atoms form atomic wires aligned along the [110] direc-
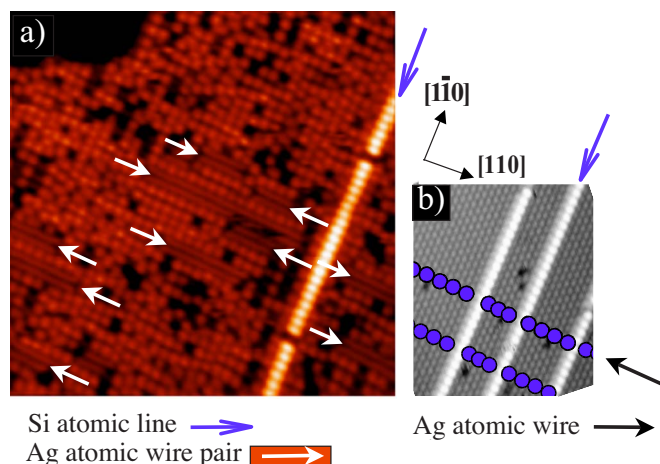
FIG. 5. (Color online) (a) 245×245 Å^2 STM topograph (filled states) of 1 ML of Ag/β-SiC(100) $c(4 \times 2)$ surface ($V_S = -3$ V, $I_t = 0.3$ nA) also showing a Si atomic line (in bright) and Ag atomic wire pairs. (b) 130×155 Å^2 STM topograph (filled states) with a schematic of Ag atomic wires connecting Si-dimer lines.

tion, i.e., perpendicular to the Si atomic wire (Fig. 5). Amazingly, some of these wires are grouped by pairs, exhibiting a degraded corrugation, as observed, e.g., on alkali metal atomic wires, making the surface metallic [Fig. 5(a)].[35,36]

IV. DISCUSSION

Our above results showing room temperature Ag atom diffusion along the Si-dimer rows support a picture of Ag weakly bound to the β-SiC(100) $c(4 \times 2)$ surface at pedestal sites. While such diffusion occurs randomly for isolated Ag atoms, the Ag-Ag interaction becomes dominant when the distance between Ag atoms decreases with attractive Ag-Ag atom interactions. The Ag atom interaction with the $c(4 \times 2)$ surface remains slightly weaker with no Si alloy formation.[3–6] However, the initial Ag interaction with surface Si atoms is significant enough to have the Si-dimer rows acting as "atomic rails" for the Ag atoms.

Interestingly, theoretical calculations for the Ag-Si(100) 2×1 system suggest that the Ag atoms do not diffuse along the Si-dimer rows but perpendicularly,[32] in contrast to the situation occurring here on the β-SiC(100) $c(4 \times 2)$ surface. Indeed, Si-dimer flipping is predicted to act as an atomic migration barrier along the dimer rows for the Si(100) 2×1 surface.[32] This is not the case here, with no dimer flipping taking place at room temperature.[16–18] However, the situation is totally different at higher temperatures since a $c(4 \times 2)$ to 2×1 phase transition occurs.[37] In such a transition, Si-Si dimer vibrations are occurring for both up and down dimers of the AUDD arrangement, leading to the dimers to all have the same average height in a dynamic situation.[37] In this case, the migration barrier along the dimer rows for Ag atoms is likely to increase significantly, in agreement with predictions made for the Si(100) 2×1.[32] Since the Ag atom diffusion will also increase with the temperature, the Ag atoms remaining on the surface (i.e., not desorbed upon annealing) would have a migration direction perpen-

dicular to the dimer rows, in contrast to the situation occurring at room temperature. This is precisely observed here in Fig. 4, with Ag atoms forming atomic wires or stripes along the [110] direction. At this stage, it might be of interest to compare with Si deposition on Si(100). In this case, both room and high temperature depositions lead to the formation of Si islands with atoms preferentially aligned perpendicularly to the dimer rows.[38] By postannealing (around 600 °C), the shape of the Si islands becomes more isotropic, suggesting that the as-deposited islands are in a nonequilibrium state; the Si atoms' preferential alignment perpendicular to the dimer rows is believed to result from an anisotropic lateral accommodation coefficient.[38] This is in contrast to the Ag/β-SiC(100) system for which annealing at 600 °C results in the partial removal of Ag atoms and 1D nanostructures perpendicular to dimer rows. This very interesting feature potentially allows the selective nanofabrication of metal atomic wires on a terrace and not only at step edges, as observed, e.g., for Au on Si(100).[39] In addition, such Ag atomic wire fabricated at 600 °C temperature could be used as a "bridge" between the Si-Si dimer wires that self-organized on this $c(4 \times 2)$ surface and are stable up to 900 °C, as shown in a schematic [Fig. 5(b)].[16,17] This potentially opens up cross-wiring for these interesting nano-objects, allowing connecting two adjacent Si atomic lines.

It is now interesting to correlate the present results to the molecular hydrogen (H$_2$) interaction with the same β-SiC(100) 3×2 and $c(4 \times 2)$ surface reconstructions with major differences occurring between these two surfaces.[40] Amazingly enough, the 3×2 reconstruction has been shown to be almost totally inert to molecular H$_2$, while instead, the $c(4 \times 2)$ surface is found to be highly reactive (8 orders of magnitude higher when compared to silicon), with molecular dissociation readily taking place on the latter.[40] In addition, H atoms are subsequently found to diffuse along the Si-Si dimer rows of the $c(4 \times 2)$ surface at room temperature,[40] just like the Ag atoms do, as described above. In both cases, the 3×2 surface is almost not reactive with the adsorbate with no H$_2$ sticking and a weak Ag atom-surface interaction, leading to Ag-Ag interaction to be the driving force in the observed silver cluster formation. Recently, a theoretical investigation has brought additional insights into the understanding of H$_2$ interaction with the 3×2 and $c(4 \times 2)$ reconstructions of the β-SiC(100) surface.[41] This study predicts that H$_2$ interaction with the surface is taking place for intradimer molecular adsorption sites (i.e., between two neighboring dimers belonging to the same row), which is found to be favorable on the $c(4 \times 2)$ and precisely not on the 3×2 reconstruction.[41] Interestingly, this situation is similar for the Ag atoms with pedestal adsorption sites, i.e., between two neighboring dimers belonging to the same row. Notice that, as group I elements (hydrogen and alkali metals), the Ag atom has a single s electron valence orbital ($5s$) having an extended wave function. Since the $c(4 \times 2)$ is a "more polar" surface compared to the 3×2 reconstruction, one can therefore easily imagine that the interaction with the surface would be easier for a charge transfer as, e.g., the case of other full d-band metal (such as Au) on polar compound semiconductor surfaces.

V. CONCLUSIONS

In conclusion, while 3D Ag cluster formation is found on the β-SiC(100) 3×2 reconstruction as a result of dominant Ag-Ag interaction at room temperature with no surface wetting, an on-site Ag atoms pedestal adsorption occurs on the $c(4 \times 2)$ surface. At 25 and 600 °C, Ag atom diffusion is highly anisotropic, occurring along and perpendicular to the dimer rows, respectively. Flipping dimer acting as a diffusion barrier along the dimer rows, at high temperatures is likely at the origin of this very interesting behavior. It allows 1D Ag atomic wire and stripe nanoengineering on a wide band gap semiconductor surface, minimizing bulk conductivity, which opens advantageous prospects in various fields such as transport property investigations or cross-wiring in neural networks of massively parallel atomic lines.

*On leave from Russian Academy of Sciences, Chernogolovka, Moscow District, Russia.

[1] C. T. Campbell, Surf. Sci. Rep. **27**, 1 (1997).

[2] A. Christensen, A. V. Ruban, P. Stoltze, K. W. Jacobsen, H. L. Skriver, J. K. Nørskov, and F. Besenbacher, Phys. Rev. B **56**, 5822 (1997).

[3] G. Le Lay, V. Yu. Aristov, L. Seehofer, T. Buslaps, R. L. Johnson, M. Gothelid, M. Hammar, U. O. Karlsson, S. A. Flodström, R. Feidenhans'l, M. Nielsen, E. Findeisen, and R. I. G. Uhrberg, Surf. Sci. **307**, 280 (1994).

[4] Shih Hung Chou, A. J. Freeman, S. Grigoras, T. M. Gentle, B. Delley, and E. Wimmer, J. Am. Chem. Soc. **109**, 1880 (1987).

[5] M. Hanbücken, T. Doust, O. Osasona, G. Le Lay, and J. A. Venables, Surf. Sci. **168**, 133 (1986).

[6] G. Le Lay, Surf. Sci. **132**, 169 (1983).

[7] R. J. Wilson and S. Chiang, Phys. Rev. Lett. **58**, 369 (1987); **59**, 2329 (1987).

[8] S. Hasegawa, X. Tong, S. Takeda, N. Sato, and T. Nagao, Prog. Surf. Sci. **60**, 89 (1999).

[9] W. Chen, A. Kahn, P. Soukiassian, P. S. Mangat, J. Gaines, C. Ponzoni, and D. Olego, J. Vac. Sci. Technol. B **12**, 2639 (1994); Phys. Rev. B **51**, 14265 (1995).

[10] H. Engelhard, J. A. Schäfer, F. Stietz, A. Goldmann, R. Fellenberg, and W. Braun, Surf. Sci. **276**, 21 (1992).

[11] H. Engelhard, F. Stietz, S. Sloboshanin, V. Persch, Th. Allinger, J. A. Schäfer, and A. Goldmann, Appl. Surf. Sci. **90**, 89 (1995).

[12] S. Sloboshanin, H. Engelhard, A. Goldmann, and J. A. Schäfer, Appl. Surf. Sci. **143**, 104 (1999).

[13] *Silicon Carbide, A Review of Fundamental Questions and Applications to Current Device Technology*, edited by W. J. Choyke, H. M. Matsunami, and G. Pensl (Akademie, Berlin, 1998), Vols. I and II.

[14] V. M. Bermudez, Phys. Status Solidi B **202**, 447 (1997).

[15] J. Pollmann and P. Krüger, J. Phys.: Condens. Matter **16**, S1659(2004).

[16] P. Soukiassian and H. Enriquez, J. Phys.: Condens. Matter **16**, S1611 (2004).

[17] P. Soukiassian, F. Semond, A. Mayne, and G. Dujardin, Phys. Rev. Lett. **79**, 2498 (1997).

[18] L. Douillard, V. Yu. Aristov, F. Semond, and P. Soukiassian, Surf. Sci. Lett. **401**, L395 (1998).

[19] P. Soukiassian, V. Derycke, F. Semond, and V. Yu. Aristov, Microelectron. J. **36**, 969 (2005).

[20] F. Semond, P. Soukiassian, A. Mayne, G. Dujardin, L. Douillard, and C. Jaussaud, Phys. Rev. Lett. **77**, 2013 (1996).

[21] W. Lu, P. Krüger, and J. Pollmann, Phys. Rev. B **60**, 2495 (1999).

[22] M. D'angelo, H. Enriquez, V. Y. Aristov, P. Soukiassian, G. Renaud, A. Barbier, M. Noblet, S. Chiang, and F. Semond, Phys. Rev. B **68**, 165321 (2003).

[23] A. Tejeda, D. Dunham, F. J. García de Abajo, J. D. Denlinger, E. Rotenberg, E. G. Michel, and P. Soukiassian, Phys. Rev. B **70**, 045317 (2004).

[24] P. Soukiassian, F. Semond, L. Douillard, A. Mayne, G. Dujardin, L. Pizzagalli, and C. Joachim, Phys. Rev. Lett. **78**, 907 (1997).

[25] V. Derycke, P. Fonteneau, and P. Soukiassian, Phys. Rev. B **62**, 12660 (2000).

[26] A. Catellani, G. Galli, F. Gygi, and F. Pellacini, Phys. Rev. B **57**, 12255 (1998).

[27] L. Douillard, F. Semond, V. Yu. Aristov, P. Soukiassian, B. Delley, A. Mayne, G. Dujardin, and E. Wimmer, Mater. Sci. Forum **264-268**, 379 (1998).

[28] V. Y. Aristov, P. Soukiassian, A. Catellani, R. Di Felice, and G. Galli, Phys. Rev. B **69**, 245326 (2004).

[29] A. Tejeda, E. Wimmer, P. Soukiassian, D. Dunham, E. Rotenberg, J. D. Denlinger, and E. G. Michel, Phys. Rev. B **75**, 195315 (2007).

[30] D. W. Niles, H. Höchst, G. W. Zajac, T. H. Fleisch, B. C. Johnson, and J. M. Meese, J. Appl. Phys. **65**, 662 (1989).

[31] N. Rodriguez, M. D'angelo, V. Yu. Aristov, and P. Soukiassian, Mater. Sci. Forum **435**, 587 (2003).

[32] R. H. Zhou, P. L. Cao, and L. Q. Lee, Surf. Sci. Lett. **290**, L649 (1993).

[33] K.-J. Kong, H. W. Yeom, D. Ahn, H. Yi, and B. D. Yu, Phys. Rev. B **67**, 235328 (2003).

[34] P. Soukiassian, *Fundamental Approach to New Materials Phases-Ordering at Surfaces and Interfaces*, Springer Series in Materials Science Vol. 17 (1992), p. 197.

[35] V. Derycke, P. Fonteneau, Y. K. Hwu, and P. Soukiassian, Appl. Phys. Lett. **88**, 022105 (2006).

[36] P. Soukiassian, J. A. Kubby, P. Mangat, Z. Hurych, and K. M. Schirm, Phys. Rev. B **46**, 13471 (1992).

[37] V. Y. Aristov, L. Douillard, O. Fauchoux, and P. Soukiassian, Phys. Rev. Lett. **79**, 3700 (1997).

[38] Y. W. Mo, B. S. Swartzentruber, R. Kariotis, M. B. Webb, and M. G. Lagally, Phys. Rev. Lett. **63**, 2393 (1989).

[39] R. Losio, K. N. Altmann, A. Kirakosian, J.-L. Lin, D. Y. Petrovykh, and F. J. Himpsel, Phys. Rev. Lett. **86**, 4632 (2001).

[40] V. Derycke, P. Fonteneau, N. P. Pham, and P. Soukiassian, Phys. Rev. B **63**, 201305(R) (2001).

[41] Xiangyang Peng, P. Krüger, and J. Pollmann, Phys. Rev. B **75**, 073409 (2007).